

# CHEMISTRY

## A European Journal

A Journal of



### Accepted Article

**Title:** Synergistic Hydrogenation over Palladium through the Assembly of MIL-101(Fe) MOF over Palladium Nanocubes

**Authors:** Vasudeva Rao Bakuru and Suresh Babu Kalidindi

This manuscript has been accepted after peer review and appears as an Accepted Article online prior to editing, proofing, and formal publication of the final Version of Record (VoR). This work is currently citable by using the Digital Object Identifier (DOI) given below. The VoR will be published online in Early View as soon as possible and may be different to this Accepted Article as a result of editing. Readers should obtain the VoR from the journal website shown below when it is published to ensure accuracy of information. The authors are responsible for the content of this Accepted Article.

**To be cited as:** *Chem. Eur. J.* 10.1002/chem.201704119

**Link to VoR:** <http://dx.doi.org/10.1002/chem.201704119>

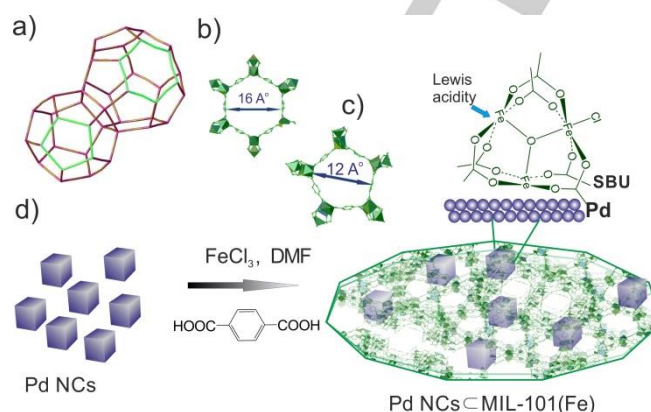
Supported by  
**ACES**

WILEY-VCH

# Synergistic Hydrogenation over Palladium through the Assembly of MIL-101(Fe) MOF over Palladium Nanocubes

Vasudeva Rao Bakuru<sup>[a],[b]</sup> and Suresh Babu Kalidindi<sup>\*[a]</sup>

**Abstract:** Enhancing catalytic performance of metal nanoparticles is highly sought for many industrial catalytic processes. In this regard, assembling of crystalline porous super-tunable metal-organic frameworks (MOFs) around preformed metal nanoparticles is an attractive prospect as this strongly influences the activity of the entire nanoparticle surface. Herein, we assembled MIL-101(Fe) MOF onto the Pd nanocubes and evaluated the catalytic properties of the hybrid material using hydrogenation of variety of  $\alpha,\beta$ -unsaturated carbonyl compounds; namely cinnamaldehyde, crotonaldehyde and  $\beta$ -ionone. Owing to the synergistic effects originated from the Lewis acid sites present on MOF and Pd active sites, striking improvements in the activities and selectivities were observed for Pd-MIL-101(Fe) hybrid material. The turn over frequency (TOF) values increased up to ~20 folds and for all three substrates under study C=C preferentially got hydrogenated over C=O. Furthermore, the Pd-MIL-101(Fe) catalyst was readily reusable and highly stable.



**Scheme 1.** a) shows MTN topology of MIL-101(Fe) MOF; the hexagonal and pentagonal window openings are shown in b) and c); d) shows schematic representation of Pd-MIL-101 architecture formation.

Transition metal nanoparticles (NPs) are widely employed in many industrial catalytic processes which include fine chemical manufacturing, polymer synthesis, and energy conversion.<sup>[1]</sup> The catalytic properties majorly stems from the large percentage of uncoordinated surface atoms present on the surface of NPs. Rational tuning of the catalytic properties and preventing the aggregation of NPs during reaction conditions are the two major endeavors in this area. In this regard, recently fabrication of metal-porous matrix architectures wherein metal surface is completely covered with porous matrix has emerged as a new promising approach.<sup>[2]</sup> Here, the porous matrix not only prevent the aggregation of NPs but also provides the platform for the tuning of catalytic properties via confinement/electronic effects present at the interface between metal and matrix.

Well-defined porous crystalline materials such as metal-organic frameworks (MOFs) will be advantageous as matrix as they offer exceptional control over the pore surface chemistry.<sup>[3]</sup> MOFs are formed by the coordination linkage between organic linker/ligand and metal ions/metal clusters (secondary building units, SBUs).<sup>[4]</sup> Though, various metal-MOF nanocomposites with different nanostructure are known,<sup>[5]</sup> metal-MOF architectures<sup>[6]</sup> wherein MOFs are assembled on to the preformed metal NPs are chosen for the present study to strongly influence the activity of the entire nanoparticle surface. These architectures have various apparent advantages (Table S1) which include i) sieving of reactant molecules through MOF matrix,<sup>[6a,c,e,f]</sup> ii) modulation of electronic structure of metal active sites through the charge transfer between SBU and metal

NP surface,<sup>[7a]</sup> iii) increased reactants concentration around metal active centers due to favorable adsorption of reactant molecules into MOF pores,<sup>[8]</sup> iv) catalytic synergy due to the additional active sites present on MOF matrix, v) modulating the chemical environment around active center by virtue of ability to systematically tune the pore surface chemistry of the MOF.<sup>[9]</sup> It is intriguing to note that only limited studies are reported demonstrating few of these advantages. The Pd NPs which are excellent hydrogenation catalysts have been incorporated in the pores of MOFs and/or supported on the exterior surfaces of MOFs.<sup>[10]</sup> Especially, MIL-101 MOFs are widely used as support/host because of its stability against water and wide pore openings.<sup>[11]</sup> However, efforts to grow MOFs on preformed Pd NPs are still scarce,<sup>[12]</sup> [7a] especially synergetic effects arising out of such architecture are yet to be comprehensively evaluated.

In this context, we have grown MIL-101(Fe) MOF<sup>[13]</sup> {Fe<sub>3</sub>OCl [(O<sub>2</sub>C)-C<sub>6</sub>H<sub>4</sub>-(CO<sub>2</sub>)<sub>3</sub>(H<sub>2</sub>O)<sub>2</sub>]<sub>3</sub>·nH<sub>2</sub>O} on preformed Pd nanocubes (NCs) to generate a bifunctional catalyst with Pd active centers on the metal nanoparticle and Lewis acid centers on SBUs of MOF. The cooperative catalytic properties aroused out of this combination of active sites were established for the hydrogenation of  $\alpha,\beta$ -unsaturated carbonyl compounds i.e. cinnamaldehyde, crotonaldehyde, and  $\beta$ -ionone. Remarkably, significant improvement in the activities and selectivities were noted before and after coating Pd NCs with MIL-101(Fe) MOF. The turn over frequency (TOF) values increased up to ~20 folds.

The Pd NCs were synthesized (Figure S1) from Na<sub>2</sub>PdCl<sub>4</sub> by using ascorbic acid as reducing agent, PVP as stabilizer and KBr as a shape directing agent.<sup>[14]</sup> MIL-101(Fe) was coated on preformed Pd NCs (~80 mg) by storing in DMF at 120 °C for 12 h in the presence of terephthalic acid (0.7 mmol) and FeCl<sub>3</sub> (0.7 mmol). The brown solid was isolated and washed with fresh DMF and ethanol. The powder X-ray diffraction (PXRD) data (Figure 1a) of the as-synthesized solid confirms the presence of both MIL-101(Fe) and Pd face centered cubic crystalline phases in the material. The Pd crystallite size calculated from PXRD

[a] V. R. Bakuru, S. B. Kalidindi  
Materials science division, Poornaprajna Institute of Scientific  
Research, Devanahalli, Bangalore Rural 576164, India.  
Email: sureshk@poornaprajna.org

[b] V. R. Bakuru  
Graduate Studies, Manipal University, Manipal-576104, India

Supporting information for this article is given via a link at the end of the document

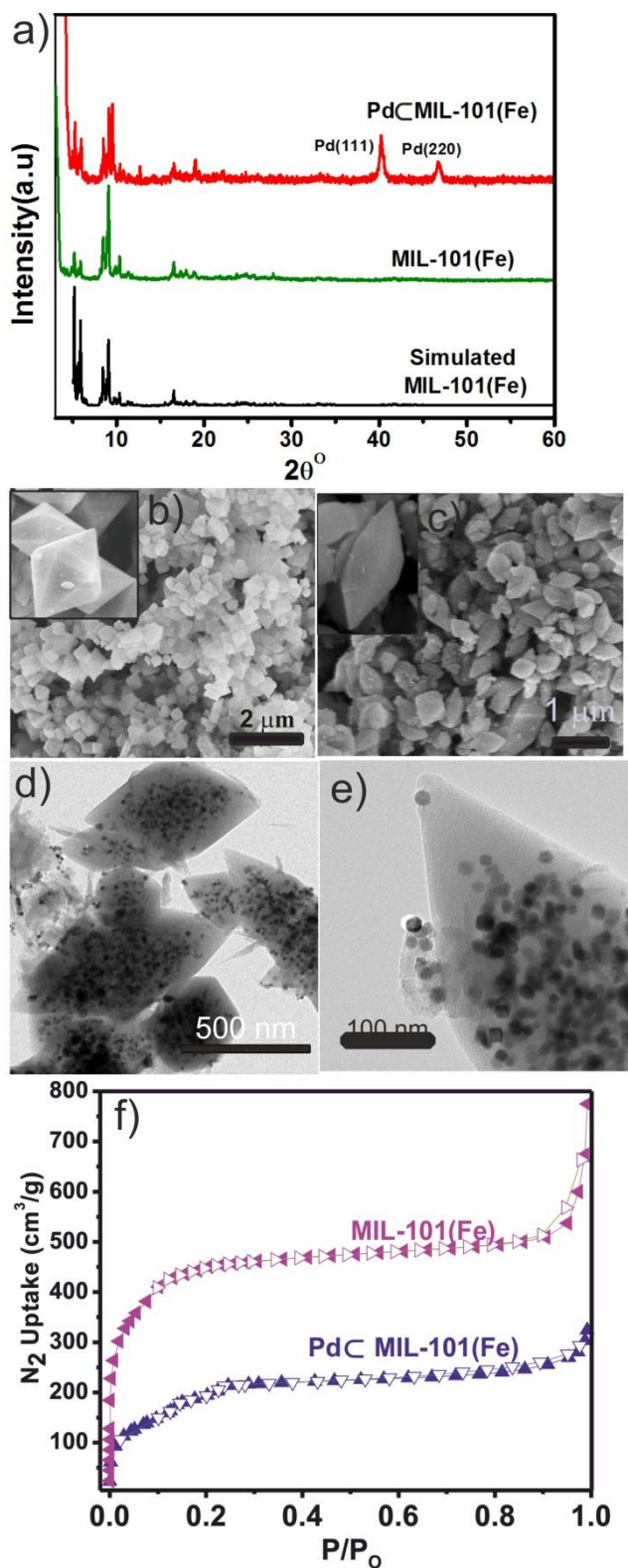


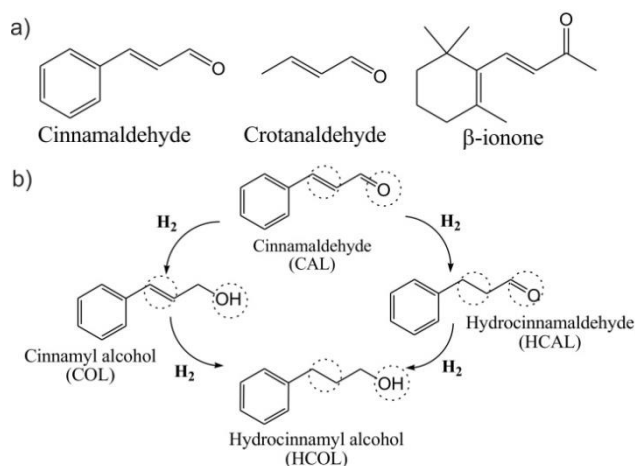
**Figure 1.** a) Powder XRD patterns of simulated and as-synthesized MIL-101(Fe) and Pd/MIL-101(Fe) samples; b) and c) scanning electron microscopy (SEM) images of MIL-101(Fe) and Pd/MIL-101(Fe) materials; d) and e) bright field-TEM images of Pd/MIL-101(Fe) catalyst; and f)  $N_2$  adsorption isotherms of Pd NCs and Pd/MIL-101(Fe).

data using Scherrer equation was 12.3 nm. The scanning

electron microscopy (SEM) analysis of the MOF samples showed particles with well-defined morphologies, octahedral for MIL-101(Fe) and spindle like elongated octahedral for Pd/MIL-101(Fe) (Figure 1b,1c). The fact that we did not observe isolated phases of Pd NCs and MOF in Pd/MIL-101(Fe) materials rules out the formation of physical mixture. This was further confirmed by transmission electron microscopy (TEM) analysis. The bright field-TEM images of Pd/MIL-101(Fe) samples revealed the presence of MOF matrix around Pd NCs (Figure 1d). As evident from the images almost all the Pd NCs are clearly embedded inside MOF matrix. Very few particles are seen near the surface with partial encapsulation (figure 1e). The average particle size was found to be  $12.5 \pm 0.8$  nm which is in good agreement with the crystallite size calculated using PXRD data. This shows that majority of Pd NCs are single crystalline in nature. The distribution of MIL-101(Fe) over various Pd NCs is also evident from scanning transmission electron microscopy energy dispersive X-ray (STEM-EDX) data (Figure S2), throughout the line scan Fe signal is present. The variations in Pd signal is in accordance with the location of Pd NCs. The weight percentage of Pd in the Pd/MIL-101(Fe) sample was estimated to be 59.5 % using inductively coupled plasma optical emission spectrometry. The samples were analysed for porosity using  $N_2$  sorption measurements at 77 K (Figure 1f). The BET surface areas of neat MIL-101(Fe) and Pd/MIL-101(Fe) were found to be  $1387$   $m^2/g$  and  $536$   $m^2/g$ , respectively. A decrease of 61% in the surface area is attributed to the 59.5 wt% of Pd content in Pd/MIL-101(Fe) material. Thermo gravimetric analysis (TGA) revealed that Pd/MIL-101(Fe) is stable up to  $280$   $^\circ C$  which is about  $50$   $^\circ C$  less compared to pristine MOF (Figure S3). The X-ray photo electron spectroscopy (XPS) analysis (Figure S4) showed that electronic structure of Pd remains unchanged before and after MOF coating on Pd NCs. The positions of  $Pd_{3/2}$  and  $Pd_{5/2}$  peaks remained same. It should be noted that at metal-MOF interface charge transfer is possible and has been observed in few metal-MOF hybrid materials.<sup>[7]</sup>

To explore the possible catalytic synergy that can originate out of the presence of Lewis acid centers and Pd active sites in Pd/MIL-101(Fe), hydrogenation of  $\alpha$ ,  $\beta$ -unsaturated carbonyl compounds (Scheme 2a.) was carried out. Hydrogenated products of  $\alpha$ ,  $\beta$ -unsaturated carbonyl compounds are widely used in perfume industry.<sup>[15]</sup> However, achieving high yields under mild conditions with good chemo- and regio- selectivities is a challenge for this class of reactions as multiple products are formed due to the hydrogenation of  $C=C$  and/or  $C=O$ . The possible hydrogenated products of CAL are shown in Scheme 2b.

We carried out hydrogenation of CAL in a Fischer bottle in isopropanol solvent under 3 bar  $H_2$  pressure in the presence of 1.5 wt% (Pd relative to the reactant) catalyst at  $40$   $^\circ C$ . The superior hydrogenation ability of Pd/MIL-101(Fe) compared to Pd NCs is evident from the 2 folds increase (to  $991.2 \pm 26.1$   $h^{-1}$  from  $469.6 \pm 10.4$   $h^{-1}$ , at  $\sim 21\%$  conversion) in TOF values. To confirm that indeed MOF coating is responsible for the enhancement of catalytic activity, we compared the activities with Pd+MOF physical mixture and Pd NCs supported on MIL-101(Fe) catalysts. As shown in Figure 2a and Figure 2b, Pd/MIL-101(Fe) catalyst outperforms all the other catalysts in terms of activity and selectivity.



**Scheme 2.** a) Selected  $\alpha,\beta$ -unsaturated carbonyl compounds for study; b) Possible products from hydrogenation of cinnamaldehyde

This emphasizes the fact that the observed catalytic properties of Pd@MIL-101(Fe) are not simple linear combination of individual counterparts but due to the synergetic effects that arise out of metal@MOF architecture. Complete conversion of CAL was noted for both Pd NCs and Pd@MIL-101(Fe) after 1.5 h of reaction time (Scheme S5). Over Pd NCs, the selectivities of saturated aldehyde HCAL and saturated alcohol HCOL were found to be 34.4 % and 65.6 %, respectively. This shows that both C=C and C=O readily got hydrogenated over Pd NCs. In contrast, Pd@MIL-101(Fe) catalyst showed preference for C=C over C=O. The selectivities of HCAL and HCOL were found to be 86.4 % and 13.6 %, respectively at 100 % conversion. This is one of the rare examples in which HCAL selectivity as high as 86.4 % is observed for Pd particle size regime of > 10 nm (Table S2). It is well documented in the literature that the  $\eta^4(\text{di-}\pi)$  mode of CAL is responsible for the formation of HCOL (Scheme S3).<sup>[16], [17]</sup> But, over Pd@MIL-101(Fe), CAL can readily bind to Fe(III) Lewis acid centers of MIL-101 through C=O group.<sup>[7c]</sup> The presence of Lewis acid centers in Pd@MIL-101(Fe) was confirmed using  $\text{NH}_3$ -temperature programmed desorption analysis (Figure S9). As C=O can participate in these secondary interactions, CAL is less likely to participate in planar  $\eta^4(\text{di-}\pi)$  kind of mode. In this scenario, the most likely adsorption reported in the literature (Table S2) for CAL hydrogenation. These findings indicate that MIL-101 effectively enhances the catalytic performance of Pd NCs in Pd@MIL-101(Fe) material. Moreover, Pd@MIL-101(Fe) catalyst was readily reusable (Figure 2c) and highly stable (Figure S7), both conversion and chemoselectivity remained almost unaltered up to 5 cycles. Hot filtration test (Figure S6) carried out by removing the catalyst after 20 min of reaction time confirms that catalysis is heterogeneous in nature.

Further, hydrogenation of crotonaldehyde (Scheme S1) and  $\beta$ -ionone (Scheme S2) was carried out over Pd NCs and Pd@MIL-101(Fe) under same reaction conditions as CAL. Reinforcing positive effect of MOF coating on Pd NCs catalytic performance, the catalysts display TOF (below 20% conversion) of  $2268.8 \pm 59.9 \text{ h}^{-1}$  and  $9837.6 \pm 134.3 \text{ h}^{-1}$  for Pd NCs and Pd@MIL-101(Fe), respectively. Similar effect is also noticed for

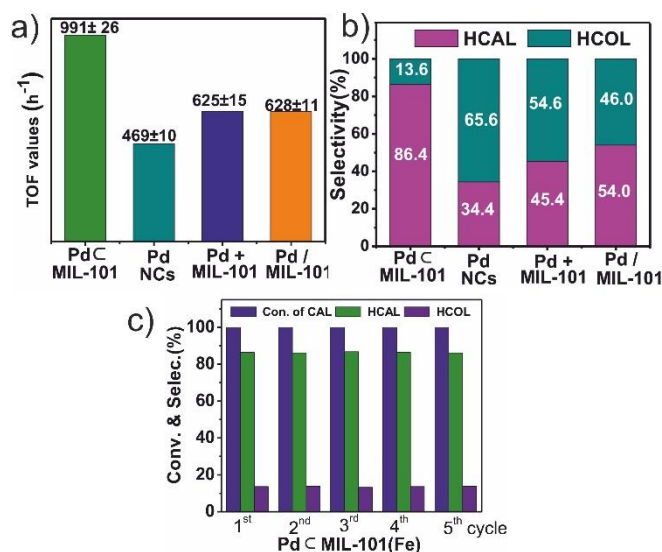


**Figure 2.** a) and b) activity and products selectivity (at 100% conversion) for the cinnamaldehyde hydrogenation over Pd@MIL-101(Fe), Pd NCs, Pd+MIL-101 (physical mixture) and Pd/MIL-101 (supported) catalysts; c) Recyclability of Pd@MIL-101(Fe) for hydrogenation of cinnamaldehyde

hydrogenation of another important fragrance chemical, i.e.  $\beta$ -ionone. The TOFs increased by 20 folds and the values were  $42.2 \pm 0.7 \text{ h}^{-1}$  and  $830.1 \pm 19.1 \text{ h}^{-1}$  for Pd NCs and Pd@MIL-101(Fe), respectively. For both substrates, Pd NCs and Pd@MIL-101(Fe) showed 100% selectivity towards only C=C hydrogenated products.

The facile hydrogenation of  $\alpha,\beta$ -unsaturated carbonyl compounds over Pd@MIL-101(Fe) might be due to presence of nanoreactors (MOF pores) around Pd active sites wherein both substrate and  $\text{H}_2$  should be relatively more localized due to the favorable interaction with Lewis acid centers and Pd active sites, respectively. The  $\text{H}_2$  adsorption measurements were performed over the catalysts under study at 298 K (Figure S8). The Pd@MIL-101(Fe) catalyst shown ~30 % higher  $\text{H}_2$  uptake compared Pd NCs and Pd/MOF. It is consistent with earlier reports that MOF coating has pronounced positive effect on the hydrogen storage properties of Pd in Pd@MOF core-shell material<sup>[7a]</sup> and accounts for the observed superior catalytic performance of the Pd@MIL-101(Fe).

In summary, the Pd NCs ( $12.5 \pm 0.8 \text{ nm}$ ) were coated with MIL-101(Fe) and its structure was confirmed by PXRD, TEM and SEM analysis. The positive effect of MOF assembly around Pd NCs clearly demonstrated for the hydrogenation of  $\alpha, \beta$ -unsaturated carbonyl compounds, TOFs increased several folds (upto 20 folds for  $\beta$ -ionone). The reusable Pd@MIL-101(Fe) catalyst also exhibited high selectivity for C=C over C=O for all the substrates. These results shows that coating of MOF onto metal NPs can enhance NPs catalytic performance remarkably due to the synergy between active centers present on metal NPs and MOF, and highlights the scope of MOFs as an encapsulating matrix.

## Acknowledgements

SBK thanks Department of science and technology(DST), Govt. of India, for funding this work under early carrier research award (ECR/2015/000350). SBK also thanks DST for INSPIRE faculty award (IFA-14/CH-166). BVR is thankful to Manipal University, India, for accepting this research as a part of a Ph.D. program.

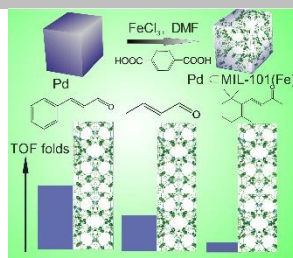
**Keywords:** Metal-Organic Frameworks (MOFs) • Metal nanoparticles • Hydrogenation • Catalysis • Hybrid materials

- [1] a) W. J. Stark, P. R. Stoessel, W. Wohlleben, A. Hafner, *Chem. Soc. Rev.* **2015**, *98*, 2035–2044; b) K. P. de Jong, *Synthesis of Solid Catalysts*, Wiley-VCH, Weinheim. **2009**; c) K. R. Kahsar, D. K. Schwartz, J. W. Medlin, *J. Am. Chem. Soc.* **2014**, *136*, 520–526.
- [2] a) Y. B. Huang, Q. Wang, J. Liang, X. Wang, R. Cao, *J. Am. Chem. Soc.* **2016**, *138*, 10104–10107; b) J.-K. Sun, W.-W. Zhan, T. Akita, Q. Xu, *J. Am. Chem. Soc.* **2015**, *137*, 7063–7066; c) J. A. Schwarz, C. I. Contescu, *Surfaces of Nanoparticles and Porous Materials*, CRC press, **1999**; d) V. Pascanu, A. Bermejo Gómez, C. Ayats, A. E. Platero-Prats, F. Carson, J. Su, Q. Yao, M. A. Pericás, X. Zou, B. Martín-Matute, *ACS Catal.* **2015**, *5*, 472–479; e) S. Goel, S. I. Zones, E. Iglesia, *J. Am. Chem. Soc.* **2014**, *136*, 15280–15290.
- [3] a) H. Kobayashi, Y. Mitsuka, H. Kitagawa, *Inorg. Chem.* **2016**, *55*, 7301–7310; b) P. Hu, J. V. Morabito, C. K. Tsung, *ACS Catal.* **2014**, *4*, 4409–4419; c) P. Falcaro, R. Ricco, A. Yazdi, I. Imaz, S. Furukawa, D. Maspoth, R. Ameloot, J. D. Evans, C. J. Doonan, *Coord. Chem. Rev.* **2015**, *307*, 237–254.
- [4] a) H. Furukawa, K. E. Cordova, M. O’Keeffe, O. M. Yaghi, *Science* **2010**, *9*, 1230444; b) H.-C. Zhou, J. R. Long, O. M. Yaghi, *Chem. Rev.* **2012**, *112*, 673–674.
- [5] a) C. Rösler, R. A. Fischer, *CrystEngComm.* **2015**, *17*, 199–217; b) C. R. Kim, T. Uemura, S. Kitagawa, *Chem. Soc. Rev.* **2016**, *45*, 3828–3845.
- [6] a) G. Lu, S. Li, Z. Guo, O. K. Farha, B. G. Hauser, X. Qi, Y. Wang, X. Wang, S. Han, X. Liu, J. S. DuChene, H. Zhang, Q. Zhang, X. Chen, J. Ma, S. C. J. Loo, W. D. Wei, Y. Yang, J. T. Hupp, F. Huo, *Nat. Chem.* **2012**, *4*, 310–316; b) T. Tsuruoka, H. Kawasaki, H. Nawafune, K. Akamatsu, *ACS Appl. Mater. Interfaces.* **2011**, *3*, 3788–3791; c) Y. Jiang, X. Zhang, X. Dai, Q. Sheng, H. Zhuo, J. Yong, Y. Wang, K. Yu, L. Yu, C. Luan, H. Wang, Y. Zhu, X. Duan, P. Che., *Chem. Mater.* **2017**, *29*, 6336–6345; d) M. Zhao, K. Deng, L. He, Yong Liu, G. Li, H. Zhao, Z. Tang, *J. Am. Chem. Soc.* **2014**, *136*, 1738–1741; e) T. Ohhashi, T. Tsuruoka, T. Matsuyama, Y. Takashima, H. Nawafune, H. Minami, K. Akamatsu, *J. Colloid Interface Sci.* **2015**, *451*, 212–215; f) C Rösler, S. Dissegna, V. L. Rechac, M. Kauer, P. Guo, S. Turner, K. Ollegott, H. Kobayashi, T. Yamamoto, D. Peeters, Y. Wang, S. Matsumura, G. Van Tendeloo, H. Kitagawa, M. Muhler, F. X. L. i Xamena, R. A. Fischer, *Chem. Eur. J.* **2017**, *23*, 3583–3594.
- [7] a) G. Li, H. Kobayashi, J. M. Taylor, R. Ikeda, Y. Kubota, K. Kato, M. Takata, T. Yamamoto, S. Toh, S. Matsumura, H. Kitagawa, *Nat. Mater.* **2014**, *13*, 802–806; b) B. Rungtaweeworant, J. Baek, J. R. Araujo, B. S. Archanjo, K. M. Choi, O. M. Yaghi, G. A. Somorjai, *Nano Lett.* **2016**, *7645–7649*; c) M. Zhao, K. Yuan, Y. Wang, G. Li, J. Guo, L. Gu, W. Hu, H. Zhao, Z. Tang, *Nature.* **2016**, *539*, 76–80; d) H. Liu, L. Chang, L. Chen, Y. Li, *Chem Cat Chem.* **2016**, *8*, 946–951.
- [8] K. Na, K. M. Choi, O. M. Yaghi, G. A. Somorjai, *Nano Lett.* **2014**, *14*, 5979–5983
- [9] K. M. Cho, K. Na, G. A. Somorjai, O. M. Yaghi, *J. Am. Chem. Soc.* **2015**, *137*, 7810–7816.
- [10] a) X. Li, Z. Guo, C. Xiao, T. W. Goh, D. Tesfagaber, W. Huang, *ACS Catal.* **2014**, *4*, 3490–3497; b) X. Li, T. W. Goh, L. Li, C. Xiao, Z. Guo, X. C. Zeng, W. Huang, *ACS Catal.* **2016**, *6*, 3461–3468; c) M. Pourkhosravani, S. Dehghanpour, F. Farzaneh, *Catal. Letters.* **2016**, *146*, 499–508; d) S. Gao, N. Zhao, M. Shu, S. Che, *Appl. Catal. A Gen.* **2010**, *388*, 196–201; e) A. Ajjaz, Q.-L. Zhu, N. Tsumori, T. Akita, Q. Xu, *Chem. Commun.* **2015**, *51*, 2577–2580; f) M. Saikia, L. Saikia, *RSC Adv.* **2016**, *6*, 14937–14947; g) A. Nagendiran, V. Pascanu, A. B. Gómez, G. G. Miera, C. i Tai, O. Verho, B. M n-Matute, J. -E. B.ckvall, *Chem. Eur. J.* **2016**, *22*, 7184 – 7189; h) L. Chen, H. Chen, Y. Li, *Chem. Commun.* **2014**, *50*, 14752–14755.
- [11] a) J. Hermannsdörfer, R. Kempe, *Chem. Eur. J.* **2011**, *17*, 8071–8077 ; b) J. Hermannsdörfer, M. Friedrich, N. Miyajima, R. Q. Albuquerque, S. Kmmel, R. Kempe, *Angew. Chem. Int. Ed.* **2012**, *51*, 11473 –11477; c) J. Hermannsdörfer, M. Friedrich, R. Kempe, *Chem. Eur. J.* **2013**, *19*, 13652–13657; d) D. Tilgner, M. Friedrich, J. Hermannsdörfer, R. Kempe, *ChemCatChem.* **2015**, *7*, 3916–3922; e) H. Ren, C. Li, D. Yin, J. Liu, C. Liang, *RSC Adv.*, **2016**, *6*, 85659–85665; f) H. Li, Z. Zhu, F. Zhang, S. Xie, H. Li, P. Li, X. Zhou, *ACS Catal.* **2011**, *1*, 1604–1612.
- [12] a) M. Zhao, K. Deng, L. He, Y. Liu, G. Li, H. Zhao, Z. Tang, *J. Am. Chem. Soc.* **2014**, *136*, 1738; b) Q. Yang, Q. Xu, S.-H. Yu, H.-L. Jiang, *Angew. Chem. Int. Ed.* **2016**, *55*, 3685.
- [13] a) G. Férey, C. Mellot-Draznieks, C. Serre, F. Millange, J. Dutour, S. Surblé, I. Margiolaki, *Science.* **2005**, *309*, 2040–2042; b) K. Taylor-Pashow, J. Rocca, *J. Am. Chem. Soc.* **2009**, *131*, 14261–14263.
- [14] B. Lim, M. Jiang, J. Tao, P. H. C. Camargo, Y. Zhu, Y. Xia, *Adv. Funct. Mater.* **2009**, *19*, 189–200.
- [15] P. Gallezot, D. Richard, *Catal. Rev. Sci. Eng.* **1998**, *40*, 81–126.
- [16] M. Polanyi; J. Horiuti, *Trans. Faraday Soc.* **1934**, *30*, 1164.
- [17] F. Delbecq and P. Sautet, *J. Catal.* **1995**, *152*, 217–236.

## Entry for the Table of Contents

## COMMUNICATION

MOF assembly around preformed Pd nanocubes enhanced the catalytic performance of Pd several folds for hydrogenation of  $\alpha$ ,  $\beta$ -unsaturated carbonyl compounds owing to synergy between functional sites present on metal nanoparticle and MOF.



Vasudeva Rao Bakuru[a],[b] and Suresh Babu Kalidindi\*[a]

**Page No. – Page No.**  
**Synergistic Hydrogenation over Palladium through the Assembly of MIL-101(Fe) MOF over Palladium Nanocubes**